

Thermodynamic and Transport Properties of CeMg_2Cu_9 under Pressure

Masakazu ITO ^{*}, Koji ASADA, Yuko NAKAMORI¹ [†], Jyun'ya HORI, Hironobu FUJII²,
Fumihiko NAKAMURA, Toshizo FUJITA and Takashi SUZUKI [‡].

Department of Quantum Matter, ADSM, Hiroshima University, Higashi-Hiroshima 739-8530 Japan

¹ *Faculty of Integrated Arts & Sciences, Hiroshima University, Higashi-Hiroshima 739-8526 Japan*

² *Natural Science Center for Basic Research and Development, Materials Science Center, Hiroshima University, Higashi-Hiroshima 739-8526 Japan*

(Received October 30, 2018)

We report the transport and thermodynamic properties under hydrostatic pressure in the antiferromagnetic Kondo compound CeMg_2Cu_9 with a two-dimensional arrangement of Ce atoms. Magnetic specific heat $C_{\text{mag}}(T)$ shows a Schottky-type anomaly around 30 K originating from the crystal electric field (CEF) splitting of the 4f state with the first excited level at $\Delta_1/k_B = 58$ K and the second excited level at $\Delta_2/k_B = 136$ K from the ground state. Electric resistivity shows a two-peaks structure due to the Kondo effect on each CEF level around $T_1^{\text{max}} = 3$ K and $T_2^{\text{max}} = 40$ K. These peaks merge around 1.9 GPa with compression. With increasing pressure, Néel temperature T_N initially increases and then change to decrease. T_N finally disappears at the quantum critical point $P_c = 2.4$ GPa.

KEYWORDS: CeMg_2Cu_9 , Specific heat, Electric resistivity, Kondo effect, Pressure effect, Crystal field effect

1. Introduction

In recent years, the studies on pressure effects on Ce based-inter metallic compounds have been carried out intensively, since the number of interesting physical properties, such as valence fluctuation,¹ non-fermi liquid^{2,3} and superconductivity,⁴⁻⁷ emerge by mean of the control physical parameters for the correlated electron systems. Especially, the discovery of superconductivity in CeRhIn_5 ,⁸ which has two dimensional alignment of the Ce atoms, attracts much attention because CeRhIn_5 has potential to provide a unique opportunity to investigate the relation between superconductivity and not only magnetism but also structural dimensionality. We believe that the two-dimensional crystal structure plays an important role for the appearance of unusual properties in the Ce-based inter metallic compounds. CeMg_2Cu_9 is one of the good candidate materials for investigating the role of the two-dimensionality with the strong correlation. This compound was firstly synthesized by Y. Nakamori *et al.*⁹ who reported that the crystal structure is the hexagonal CeNi_3 -type (space group $P6_3/mmc$).

^{*}E-mail: showa@hiroshima-u.ac.jp

[†]Present address: Institute for Materials Research, Tohoku University, Sendai 980-8577, Japan

[‡]E-mail: tsuzuki@hiroshima-u.ac.jp

The structure of this unitcell is built up by stacking of alternating MgCu₂ Laves-type and rare earth based CeCu₅-type layers along *c*-axis. The distance between the nearest Ce atoms along the *c*-axis is ~ 8.6 Å which is 1.7 times larger than that in the *c* plane (~ 5.1 Å). One can expect a two-dimensional electronic properties reflecting the two-dimensional crystal structure. In this paper, we report specific heat and electrical resistivity on CeMg₂Cu₉ under hydrostatic pressures. If in CeRhIn₅, the appearance of superconductivity by compression is related to the two dimensionality, it is interesting to search superconductivity in CeMg₂Cu₉ by compression.

2. Experimental

Polycrystalline samples of CeMg₂Cu₉ and LaMg₂Cu₉ were prepared by melting stoichiometric amount of consistent metals at 1200°C in the 0.5 MPa Ar atmosphere in a Mo-crucible. Specific heat C_P measurements were carried out by a conventional adiabatic heat-pulse method. A piston-cylinder Cu-Be clamp cell, which contains Apiezon-J oil as pressure-transmitting oil, was adopted to measure $C_P(T)$ under pressure P up to 1.0 GPa. Temperature was decreased down to 0.5 K using a ³He refrigerator. Electrical resistivity ρ were measured by a standard four-probe method in the temperature range between 2 and 300 K. We utilized two types of pressurization technique according to the range of pressure. A cubic anvil device was used for the P range between 3.0 and 8.0 GPa.^{11,12} For the $\rho(T)$ measurement in the range between 0.1 MPa and 2.3 GPa, we used a piston-cylinder type tungsten-carbide (WC) clamp cell with the equal volume mixture of Fluorinert FC70 and FC77 as the pressure transmitter. Dilution refrigerator was used to measure $\rho(T)$ from low temperature (~ 0.1 K), for 2.3 GPa.

3. Results

3.1 Specific heat

Figure 1(a) shows the temperature T dependence of specific heat $C_P(T)$ of CeMg₂Cu₉ at 10^{-4} Pa from 0.5 to 50 K together with that of the isostructural nonmagnetic LaMg₂Cu₉. A large peak which indicates the antiferromagnetic transition is observed at $T_N = 2.5$ K. Magnetic specific heat $C_{\text{mag}}(T)$ is obtained by subtraction of $C_P(T)$ of LaMg₂Cu₉ from that of CeMg₂Cu₉, which is shown in Fig. 1 (b). We roughly estimated that the Sommerfeld coefficient is not less than 117 mJ/K²mol from the value of C_{mag}/T at $T = 5$ K. A Schottky-type anomaly is found around 30 K, indicating the crystal electric field (CEF) splitting of the 4*f*-electronic levels at the Ce ion site. In the hexagonal symmetry, the sixfold degenerate state of 4*f* for Ce³⁺ splits into the three Kramers doublets. The Schottky anomaly is theoretically given by

$$C_{\text{Sc}}(T) = \frac{R}{T^2} \left[\frac{\Delta_1^2 e^{-\Delta_1/k_B T} + \Delta_2^2 e^{-\Delta_2/k_B T}}{k_B^2 Z(T)} \right]$$

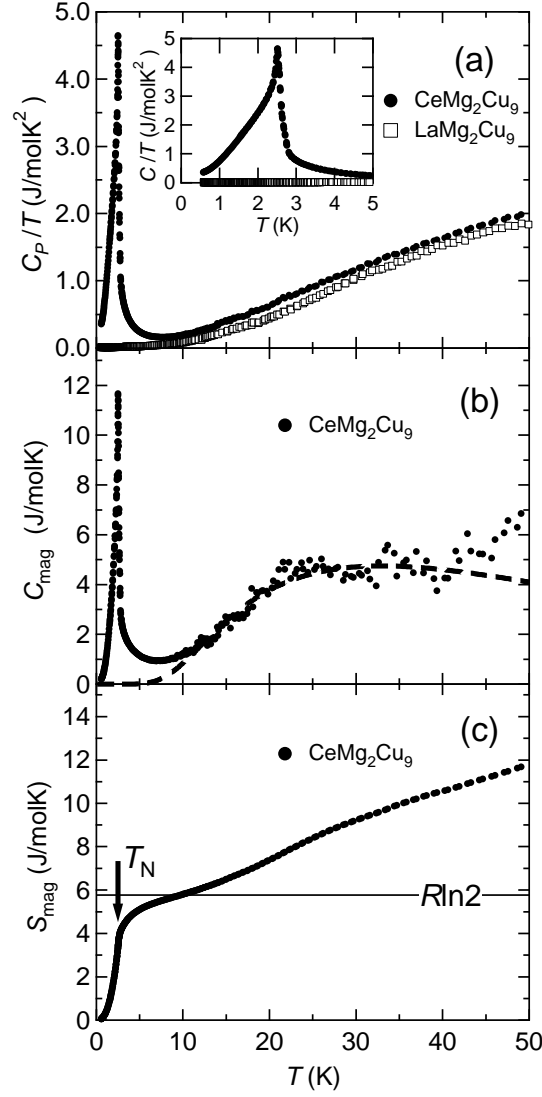


Fig. 1. (a) Temperature dependence of specific heat divided by temperature C_P/T of CeMg_2Cu_9 shown by the closed circles and LaMg_2Cu_9 in $0.5 \leq T \leq 50$ K at $P = 10^{-4}$ Pa shown by the open rectangles. (b) Temperature dependence of magnetic specific heat C_{mag} . The fitting result with eq. (1) is drawn by a broken curve. (c) Temperature dependence of the magnetic entropy S_{mag} .

$$- \left(\frac{\Delta_1 e^{-\Delta_1/k_B T} + \Delta_2 e^{-\Delta_2/k_B T}}{k_B Z(T)} \right)^2 \Big], \quad (1)$$

with $Z(T) = 1 + \exp(-\Delta_1/k_B T) + \exp(-\Delta_2/k_B T)$, where R , k_B , Δ_1 and Δ_2 are the gas constant, Boltzman factor, the first and second excited CEF energies measured from the ground level, respectively. The experimental result can be reproduced by eq. (1) with the parameters $\Delta_1/k_B = 58$ K and $\Delta_2/k_B = 136$ K as shown by the broken curve in Fig. 1(b). The magnetic

entropy $S_{\text{mag}}(T)$ is obtained by the relation

$$S_{\text{mag}}(T) = \int_0^T \frac{C_{\text{mag}}(T)}{T} dT, \quad (2)$$

and shown in Fig. 1 (c). The released S_{mag} at T_N is about 60% of $R\ln 2$, and remaining entropy ($0.4R\ln 2$) is recovered by 10 K. This suggests that the Kondo-compensated ordered moments are formed in the low temperature range. The Kondo interaction can be responsible for the entropy transfer to higher temperature.^{13,14} This is reflected in tail of C_{mag} above T_N . Figure 2 (a) displays temperature dependence of C_P/T at various pressures up to 0.91 GPa from 0.5 to 4 K. Anomalies at T_N have nearly equivalent sharpness and amplitude even for 0.91 GPa. The value of released S_{mag} at T_N is not change by pressure below 0.91 GPa as shown in Fig. 2 (b). This suggests that the Kondo-compensated ordered moments are still formed in 0.91 GPa. Figure 3 shows pressure dependence of T_N . With increasing P , T_N slightly increases up to 2.58 K at 0.89 GPa, and changes to decrease.

3.2 Electric resistivity

Temperature dependencies of the electrical resistivity $\rho(T)$ of CeMg_2Cu_9 and LaMg_2Cu_9 are plotted in Fig. 4 (a). The drop at 2.5 K, which was defined as the maximum point of $\partial\rho_{\text{mag}}/\partial T$, is due to the antiferromagnetic ordering. The magnetic contribution $\rho_{\text{mag}}(T)$ to the resistivity of CeMg_2Cu_9 was obtained by the subtracting $\rho_{\text{LaMg}_2\text{Cu}_9}$ from $\rho_{\text{CeMg}_2\text{Cu}_9}$ and is shown in the semi-logarithmic scale in Fig. 4(b). $\rho_{\text{mag}}(T)$ shows the double-peaked structure around $T_1^{\text{max}} = 3$ K and $T_2^{\text{max}} = 40$ K. Similar feature were reported for some of Ce-based heavy fermion (HF) compounds, for example, CeAl_2 ,¹⁵ CePdSi_2 ¹⁶ and CePb_3 .¹⁷ By analogy of the cases for these HF compounds, the resistivity peak at T_1^{max} may originate from the Kondo scattering with the energy scale of Kondo temperature T_K for the ground state and T_2^{max} from the Kondo scattering with higher-Kondo temperature T_K^h on the whole CEF state. For the three Kramers doublets system with the energy gaps Δ_1 ($> T_K$) and Δ_2 , the relation among T_K , T_K^h , Δ_1 and Δ_2 is described as¹⁸

$$(k_B T_K^h)^3 = \Delta_1 \Delta_2 (k_B T_K). \quad (3)$$

From the above equation we calculated $T_K \sim 8$ K with Δ_1/k_B and Δ_2/k_B determined from specific heat, where we assumed $T_K^h = T_2^{\text{max}}$. Logarithmic temperature dependencies, which are indicated by the broken lines m_1 and m_2 in Fig. 4(b), can be understood by the theoretical model by Cornut and Coqblin.¹⁹ According to their model, $-\ln(T)$ dependencies arise from the Kondo effect in the CEF levels, and $\rho_{\text{mag}}(T)$ is given by

$$\rho_{\text{mag}} = \rho_{sd} + 2AJ_{cf}^3 n_f \frac{\lambda^2 - 1}{2J + 1} \ln(k_B T/D), \quad (4)$$

where ρ_{sd} is the spin disorder resistivity, A is the constants, n_f is the density of states at the Fermi level, J_{cf} (< 0) is the exchange interaction between the conduction and localized

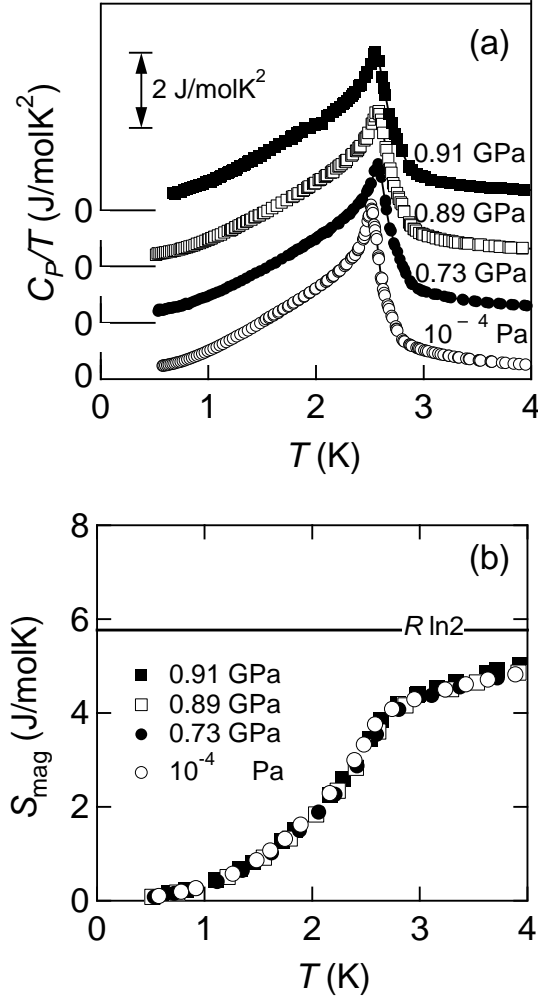


Fig. 2. Temperature dependence of (a) C_P/T and (b) S_{mag} at various pressures up to 0.91 GPa in $T \leq 4.0$ K.

$4f$ electrons, J is total angular momentum of $5/2$ for Ce^{3+} , and D is the effective band width. The parameter λ is the number of thermally accessible states, for example, $\lambda = 2$ for the ground state doublet as the low T limit and $6 (= 2J + 1)$ as the high T limit, respectively.^{19,20} The ratio of the logarithmic slopes m_2/m_1 is 4.5, and this value is close to $\rho_{\text{mag}}(\lambda = 4)/\rho_{\text{mag}}(\lambda = 2) (= 15/3)$ obtained from eq. (1) by assuming that the contribution of ρ_{sd} is small. This suggests that $-\ln(T)$ dependence m_1 and m_2 arises from the Kondo effect at the ground state ($\lambda = 2$) and the first excited state ($\lambda = 4$), respectively.¹⁹ $\rho_{\text{mag}}(T)$ measured by using the WC clamp cell in the pressure range $0.1 \text{ MPa} \leq P \leq 2.3 \text{ GPa}$ are shown in Fig. 5 (a) for some representative pressures. As expected from $C_P(T)$ above 0.89 GPa, T_N decreases with compression. T_N reduced to 0.22 K at 2.3 GPa as shown in the inset of Fig. 5 (a). T_1^{max} is almost independent of P , whereas T_2^{max} moves to lower temperatures with the

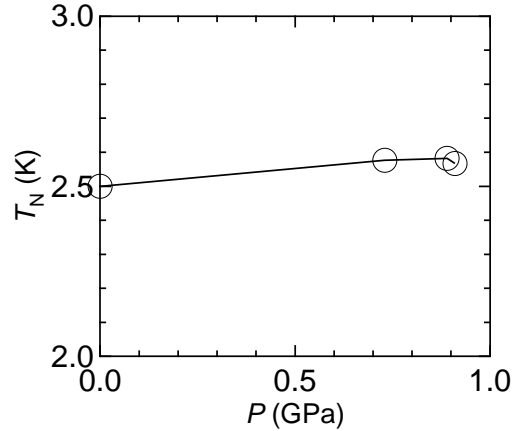


Fig. 3. Pressure dependence of T_N obtained from $C_{\text{mag}}(T)$. The solid line is guide to the eyes.

ratio $\partial T_2^{\text{max}}/\partial P \sim -17$ K/GPa and the two peaks merge at T^{max} around 1.9 GPa. T^{max} moves to higher temperature with $\partial T^{\text{max}}/\partial P \sim 20$ K/GPa above 3 GPa by compression as shown in Fig. 5 (b) which is plotted $\rho_{\text{mag}}(T)$ under P generated by the cubic anvil device in $3.0 \leq P \leq 8.0$ GPa. The negative $\partial T_2^{\text{max}}/\partial P$ observed below 1.6 GPa is unusual. According to the pressure studies on the Ce-based HF compounds, $\partial|J_{cf}n_f|/\partial P$ is to be positive,²¹ because T_K and T_K^h are in proportion to $\exp(-1/|J_{cf}n_f|)$, T_1^{max} and T_2^{max} should increase with compression as observed in CePb₃.¹⁷ It is not clear why the $\partial T_2^{\text{max}}/\partial P$ is the negative value in CeMg₂Cu₉. This unusual behavior is seen in pressure dependence of $\rho_{\text{mag}}(T)$ of CeRhIn₅ which is a pressure-induced superconductor with the 2D structure.

The effects of compression on T_N , T_1^{max} , T_2^{max} and T^{max} are summarized in Fig. 6. We can easily estimate that T_N disappears at the critical pressure $P_c = 2.4$ GPa, which is so called quantum critical point (QCP). This value is very close to the value (2.5 GPa) obtained from the resistivity measurement under pressure, which reported by Nakawaki *et al.*²² A large number of studies on QCP in the Ce-based compounds have been carried out, and some of them, for example on CePd₂Si₂,⁴ CeRh₂Si₂,⁵ and CeIn₃,⁶ find superconductivity at vicinity of the P_c in the low temperature range. In the case of CeMg₂Cu₉, we have not observed pressure-induced superconductivity around P_c so far. Many Ce-based HF superconductors have shown that pairing symmetry is anisotropic.^{23–25} When the system has an anisotropic pairing symmetry, superconducting transition temperature T_c is strongly suppressed by a small amount of impurity. We continue the search of the pressure induced superconductivity with high-quality CeMg₂Cu₉.

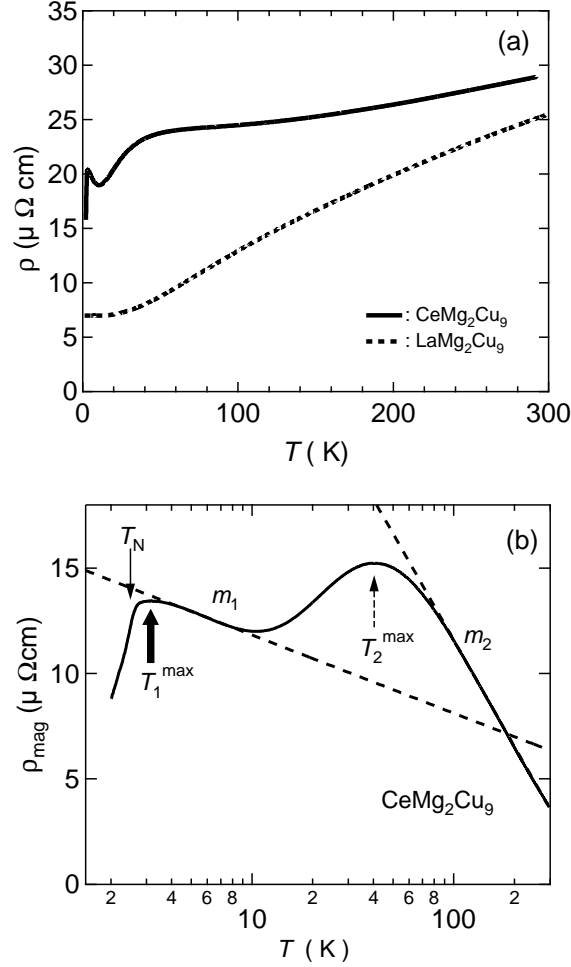


Fig. 4. (a) Temperature dependence of electrical resistivity $\rho(T)$ of CeMg_2Cu_9 presented by a solid curve and LaMg_2Cu_9 presented by a broken curve between 1.5 and 300 K at $P = 10^{-4}$ Pa. (b) Semi-logarithmic plot of magnetic resistivity $\rho_{\text{mag}}(T)$. The broken lines are guides to the eyes, indicating $-\ln T$ dependence with slope m_1 and m_2 of $\rho_{\text{mag}}(T)$. We defined Néel temperature T_N as the maximum point of $\partial\rho_{\text{mag}}/\partial T$.

4. Conclusion

We have studied on specific heat and electric resistivity under hydrostatic pressure in CeMg_2Cu_9 which has the two-dimensional Ce atoms alignment. Magnetic specific heat shows the schottky-type anomaly due to $4f$ levels of Ce^{3+} split into three Kramers doublets by crystal field effect with energy gap $\Delta_1/k_B = 58$ K and $\Delta_2/k_B = 138$ K. This crystal field splitting also affect on electric resistivity as the appearance of the two-peaks structure at $T_1^{\text{max}} = 3$ K and $T_2^{\text{max}} = 40$ K and $-\ln T$ dependencies above T_1^{max} and T_2^{max} . Analysis by the Cornut and Coqblin model, we show that the $-\ln T$ dependencies above T_1^{max} and T_2^{max} are originated from the Kondo effect on the ground and first excited state, respectively. With increasing pressure, T_2^{max} decreases, and merged with T_1^{max} around 1.9 GPa. This suggests the

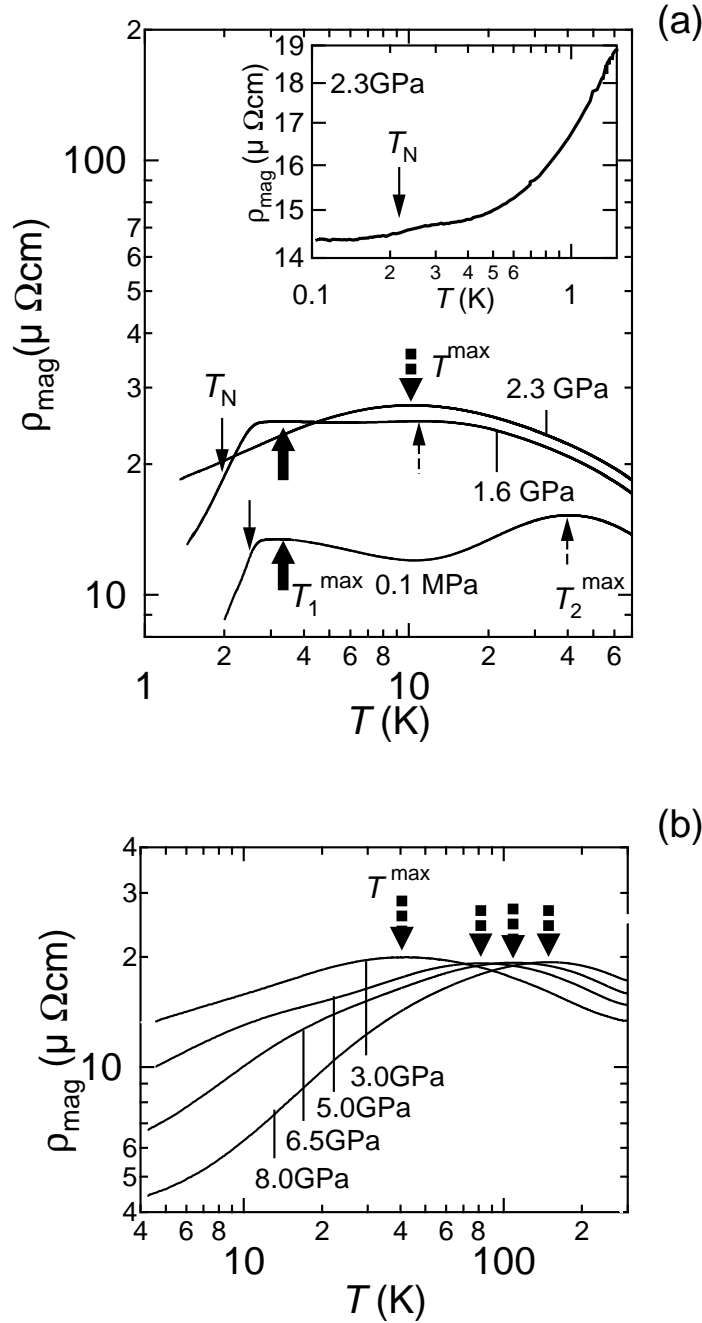


Fig. 5. Temperature dependence of electrical resistivity $\rho_{\text{mag}}(T)$ under pressures. (a) $\rho_{\text{mag}}(T)$ in the range of $1.5 \leq T \leq 70$ K and $0.1 \text{ MPa} \leq P \leq 2.3$ GPa measured using the WC clamp cell. Inset shows $\rho_{\text{mag}}(T)$ at 2.3 GPa in the range of $0.1 \leq T \leq 2$ K measured using the WC clamp cell in a dilution refrigerator. (b) $\rho_{\text{mag}}(T)$ in the range of $4.2 \leq T \leq 300$ K and $1.5 \leq P \leq 8.0$ GPa measured using the cubic-anvil device. The thin, thick, thin-broken and thick-broken arrows show the positions of Néel temperature T_N , characteristic temperatures T_1^{max} , T_2^{max} and T^{max} , respectively.

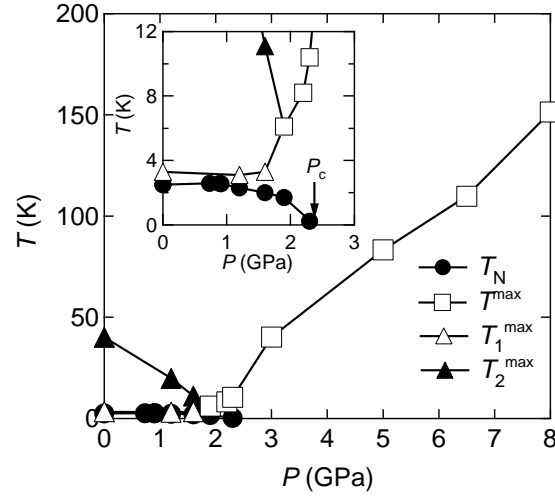


Fig. 6. Pressure dependence of the Néel temperature T_N , the characteristic temperature T_1^{\max} , T_2^{\max} and T^{\max} obtained from $C_{\text{mag}}(T)$ and $\rho_{\text{mag}}(T)$. Inset is plotted in an expanded scale in the ranges of $0 \leq T \leq 12$ K and $0 \leq P \leq 3.0$ GPa. The solid lines are guides to the eyes.

Kondo temperature T_K becomes same order of the energy level for the crystal field splitting by compression. T_N decreases with increasing pressure after having maximum 2.6 K at 0.89 GPa, and disappear at the quantum critical point $P_c = 2.4$ GPa. We also presented the Kondo temperature T_K (~ 8 K) of CeMg_2Cu_9 .

5. Acknowledgments

This work was partially supported by Grant-in-Aid for COE Research (No. 13CE2002) and a Scientific Research (B) (No. 13440114) from the Ministry of Education, Culture, Sports, Science and Technology of Japan.

References

- 1) T. Nakajima, K. Tsuji, T. Ishidate, H. Takahashi, S. Suzuki, A. Ochiai, T. Suzuki and T. Kasuya: J. Magn. Magn. Matt **47& 48** (1985) 293.
- 2) H. v. Löhneysen, T. Piet, G. Portisch, H. G. Schlager, A. Schroder, M. Sieck and T. Trappmann: Phys. Rev. Lett. **72** (1994) 3262.
- 3) K. Umeo, H. Kadowaki and T. Takabatake, Phys. Rev. B **55** (1997) R692.
- 4) F. M. Grosche, S. R. Julian, N. D. Mathur and G. G. Lonzarich: Physica B. **223+224** (1996) 50.
- 5) R. Movshovich, T. Graf, D. Mandrus, J. D. Thompson, J. L. Smith and Z. Fisk: Phys. Rev. B **53** (1996) 8241.
- 6) I. R. Walker, F. M. Grosche, D. M. Freye and G. G. Lonzarich: Physica C **282-287** (1997) 303.
- 7) E. Vargoz, P. Link, D. Jaccard, T. LeBihan and S. Heathman, Physica B **229** (1997) 225.
- 8) H. Hegger, C. Petrovic, E. G. Moshopolou, M. F. Hundley, J. L. Sarrao, Z. Fisk and J. D. Thomson: Phys. Rev. Lett **84** (2000) 4986.
- 9) Y. Nakamori, M. Ito, H. Fukuda, T. Suzuki, H. Fujii, T. Fujita and Y. Kitano: Physica B. **312-313** (2002) 235.
- 10) K. Kadir, T. Sakai and I. Uehara: J. Alloys Comp. **257** (1997)115.
- 11) N. Môri, Y. Okayama, H. Takahashi, Y. Haga and T. Suzuki, Jpn. J. Appl. Phys. Series **8**, 182 (1993).
- 12) Y. J. Hori, S. Iwata, H. Kurisaki, F. Nakamura, T. Suzuki and T. Fujita: J. Phys. Soc. Jpn. **71** (2002) 1346.
- 13) E. Bauer, M. Rotter, L. Keller, P. Fischer, M. Ellerby and K. A. McEwen: J. Phys. **6** (1994) 5533.
- 14) C. D. Bredl, F. Steglich and K. D. Schotte: Z. Phys. B **29** (1978) 327.
- 15) Y. Ônuki, F. Furukawa, T. Komatsubara: J. Phys. Soc. Jpn. **53** (1984) 2734.
- 16) J. J. Lu, C. Tien, L. Y. Jang, C. S. Wur: Physica B. **305** (2001) 105.
- 17) H. Suzuki, H. Kitazawa, T. Naka, J. Tang and G. Kido: Sol. State. Commun. **107** (1998) 447
- 18) K. Hanzawa, K. Yamada and K. Yosida: J. Magn. Magn. Matt **47& 48** (1985) 357
- 19) B. Cornut, and B. Coqblin: Phys. Rev. B **5** (1972) 4541.
- 20) M. F. Francillon, A. Percheron, J. C. Achard, O. Gorochoy, B. cornut, D. Jerome and B. Coqblin: Sol. State. Commun. **11** (1972) 845.
- 21) See, for example T. Kagayama, G. Oomi, H. Takahashi, N. Mori, Y. Ônuki, T. Komatsubara: Phys. Rev. B **44** (1991) 7690.
- 22) H. Nakawaki, Y. Inada, R. Asai, M. Yamada, T. Okubo, S. Ikeda, A. Thamizhavel, T. C. Kobayashi, R. Settai, E. Yamamoto and Y. Ônuki: J. Phys. **14** (2002) L305.
- 23) K. Ishida, Y. Kawasaki, K. Tabuchi, K. Kashima, Y. Kitaoka, K. Asayama, C. Geilbel, and F. Steglich :Phys. Rev. Lett **82** (1999) 5353.
- 24) R. A. Fisher, F. Bouquet, N. E. Phillips, M. F. Hundley, P. G. Pagliuso, J. L. Sarrao, Z. Fisk, and J. D. Thompson, Phys. Rev. B **65** (2002) 224509.
- 25) K. Izawa, H. Yamaguchi, Yuji Matsuda, H. Shishido, R. Settai and Y. Onuki: Phys. Rev. Lett. **87** (2001) 057002 .